

Atomic configuration and phase transition of Pt-induced nanowires on a Ge(001) surface studied using scanning tunneling microscopy, reflection high-energy positron diffraction, and angle-resolved photoemission spectroscopy

Izumi Mochizuki,^{*} Yuki Fukaya, and Atsuo Kawasuso*Advanced Science Research Center, Japan Atomic Energy Agency, 1233 Watanuki, Takasaki, Gunma 370-1292, Japan*

Koichiro Yaji, Ayumi Harasawa, and Iwao Matsuda

Institute for Solid State Physics, The University of Tokyo, 5-1-5 Kashiwa-no-ha, Kashiwa, Chiba 277-8581, Japan

Ken Wada and Toshio Hyodo

Institute of Materials Structure Science, High Energy Accelerator Research Organization (KEK), 1-1 Oho, Tsukuba, Ibaraki 305-0801, Japan

(Received 19 January 2012; revised manuscript received 27 March 2012; published 22 June 2012)

The atomic configuration and electronic band structure of Pt-induced nanowires on a Ge(001) surface are investigated using scanning tunneling microscopy, reflection high-energy positron diffraction, and angle-resolved photoemission spectroscopy. A previously proposed theoretical model, composed of Ge dimers on the top layer and buried Pt arrays in the second and fourth layers [Vanpoucke *et al.*, *Phys. Rev. B* **77**, 241308(R) (2008)], is found to be the fundamental structure of the observed nanowires. At low temperatures ($T < 80$ K), each Ge dimer is alternately tilted in the surface normal direction (asymmetric), causing a $p(4 \times 4)$ periodicity. At high temperatures ($T > 110$ K), each Ge dimer is flat with respect to the horizontal axis (symmetric), giving rise to $p(4 \times 2)$ periodicity. Upon the above phase transition, the electronic band dispersion related to the Ge dimers in the deeper energy region shifts to the Fermi level.

DOI: [10.1103/PhysRevB.85.245438](https://doi.org/10.1103/PhysRevB.85.245438)

PACS number(s): 61.05.jh, 68.37.Ef, 79.60.Jv

I. INTRODUCTION

Self-assembled nanowires formed on semiconducting crystal surfaces have attracted a great deal of interest as they can further our fundamental understanding of one-dimensional (1D) properties such as the non-Fermi liquid and the Peierls-type metal-insulator transition.¹ From these interests, extensive studies have been performed on surface 1D systems such as In/Si(111),²⁻⁴ Au/Si(553),(557),⁵ Y/Si(001),⁶ Au/Ge(001),⁷ and so on.

Recently, Gürlü *et al.*⁸ found that well-ordered and defectless nanowires can be formed on Ge(001) surfaces by depositing a submonolayer of Pt atoms. They proposed a structural model called “Pt dimer (PD)” model, here, as shown in Fig. 1(a). In this model, the first surface layer is covered by Pt dimers on a β terrace^{8,31} giving rise to a $p(4 \times 2)$ unit cell. The β terrace is composed of alternating Ge-Ge and Pt-Ge dimers along nanowires. van Houselt *et al.*⁹ reported that the surface periodicity changes from $p(4 \times 2)$ at room temperature to $p(4 \times 4)$ at temperatures below 77 K. They explained this phase transition as an alternate buckling of topmost Pt dimers due to the Peierls instability, since the doubling periodicity is associated with a reduction of the density of states near the Fermi level. On the other hand, Vanpoucke *et al.*¹⁰ suggested the phase transition is not due to the Peierls instability. On the basis of the results of recent research on theoretical calculations, two models have been proposed for the Pt-induced nanowires.^{11,12} Stekolnikov *et al.*^{12,13} suggested the tetramer-dimer-chain (TDC) model as shown in Fig. 1(b). In this model, the topmost layer is covered by Ge dimers and Pt atoms are placed in the second layer. The reconstructed $p(4 \times 2)$ unit cell contains 0.25 monolayers (ML) of Pt atoms. Figure 1(c) shows the nanowire (NW) model proposed by

Vanpoucke *et al.*^{10,11} In this model, the total coverage of Pt atoms is 0.75 ML and the surface periodicity is a $p(4 \times 2)$. The two Pt arrays in the second layer are bridged by the top Ge dimers. Pt atoms are also placed in the fourth layer. To explain the observation of $p(4 \times 4)$ periodicity at low temperatures, Vanpoucke *et al.* also suggested the existence of a Pt atom at site A in Fig. 1(c).¹⁰ In this case, the Pt coverage is 0.8125 ML.

Despite extensive studies using scanning tunneling microscopy/spectroscopy (STM/S) and *ab initio* calculations,⁸⁻¹⁸ the atomic configuration and the phase transition mechanism of Pt-induced nanowires on Ge(001) surfaces have not been fully elucidated. There are only a limited number of works of diffraction and photoemission studies revealing the structural and electronic properties associated with this surface. In this study, we investigated a highly ordered Pt-induced nanowires on Ge(001) surface using STM, reflection high-energy positron diffraction (RHEPD),¹⁹⁻²¹ and angle-resolved photoemission spectroscopy (ARPES).

II. EXPERIMENTAL SETUPS

The samples used in the STM and RHEPD experiments were cut from a mirror-polished flat Ge(001) wafer (0° OFF, n type, $R < 45 \Omega\text{cm}$). Those used in the ARPES experiments were cut from a vicinal Ge(001) wafer (2° OFF, n type, $R < 0.3 \Omega\text{cm}$) tilted in [110] direction, to realize uniformly oriented nanowires.²² Clean Ge(001) surfaces were prepared by a few cycles of sputtering in 800 V Ar^+ ion at 670 K for 15 min and annealing at 850 K for 10 min. Pt atoms were deposited at the rate of 0.01 ML/min at 620 K, to afford a coverage of ~ 1.2 ML [1 ML is defined as the number of Ge atoms on the ideal Ge(001) cutting plane ($\sim 6.3 \times 10^{14}$ atoms/cm²)]. The amount of deposited Pt atoms was calibrated using the

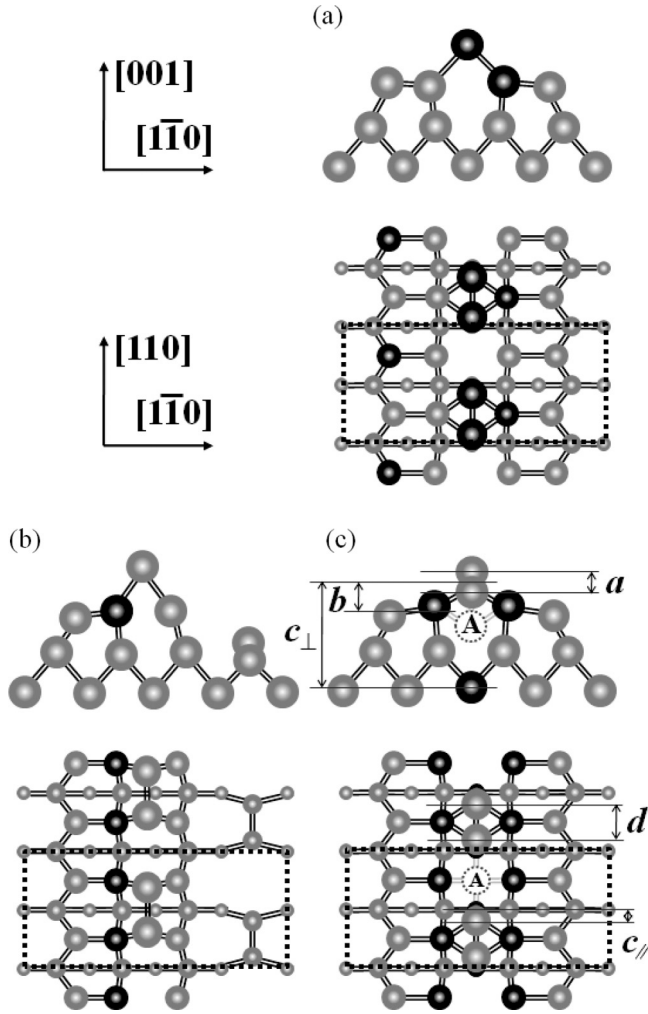


FIG. 1. Schematic illustrations of Ge(001)- $p(4 \times 2)$ -Pt structures as proposed by (a) PD, (b) TDC, and (c) NW models. The black and gray spheres represent Pt and Ge atoms, respectively. The dotted rectangles represent the $p(4 \times 2)$ unit cells. When Pt atoms are inserted at A sites, the periodicity is $p(4 \times 4)$ with a Pt coverage of 0.8125 ML. The interlayer and interatomic distances are labeled by a , b , c_{\parallel} , c_{\perp} , and d .

diffraction patterns of a Pt/Si(111) surface whose periodicity changes from 7×7 to $\sqrt{3} \times \sqrt{3}$ as the Pt coverage reaches 0.41 ML.²³ The substrate temperature was measured using infrared radiation thermometers above room temperature and thermocouples for temperatures below room temperature with an error range of ± 10 K.

STM images were obtained by using an Omicron VT-STM in the constant current mode with several tunneling currents (I) and sample bias voltages (V_S). The RHEPD experiments were performed using a positron beam of 10 keV generated from a ^{22}Na source¹⁹ at Japan Atomic Energy Agency (JAEA) and an intense positron beam in the Slow Positron Facility of the High Energy Accelerator Research Organization (KEK). The incident azimuth was set at the $[1\bar{1}0]$ direction (many-beam condition) or 22.5° away from the $[1\bar{1}0]$ direction (one-beam condition). The glancing angle (θ) was varied from 0.5° to 6° . The critical glancing angle for total reflection is approximately 2.2° as calculated from the

positron beam energy and the internal potential of a Ge crystal (2.3 eV).²⁴ The ARPES measurements were performed with polarized ultraviolet light radiation of $h\nu = 24$ eV and an angle-resolved electron analyzer (SCIENTA SES-100) at the BL-18A beamline of the KEK Photon Factory (Institute for Solid State Physics, University of Tokyo). The angular and energy resolutions were less than 1° and 0.1 eV, respectively. All the above experiments were conducted under ultra-high-vacuum ($\sim 10^{-8}$ Pa) conditions.

III. RESULTS AND DISCUSSION

A. Results of STM observations

Figure 2(a) shows an STM image obtained at room temperature. As proposed by Schäfer *et al.*,¹⁵ well-ordered Pt-induced nanowires are formed on the Ge(001) surface. The nanowire arrays cover a large area with few defects. The total area ratio of α and β terraces⁸ is less than 10%. The α terrace contains a dense defect of missing dimers related to Pt atoms sitting in subsurface positions, where the nanowires are not constructed. As shown in Figs. 2(b) and 2(c), $p(4 \times 4)$ periodicity observed at 50 K changes to $p(4 \times 2)$ at 100 K. The $p(4 \times 2)$ periodicity is preserved at room temperature. Figures 2(e) and 2(f) show the height profiles of the nanowires under the black solid lines in Figs. 2(b) and 2(c). At 50 K, the two dimers in each unit cell are tilted opposite each other

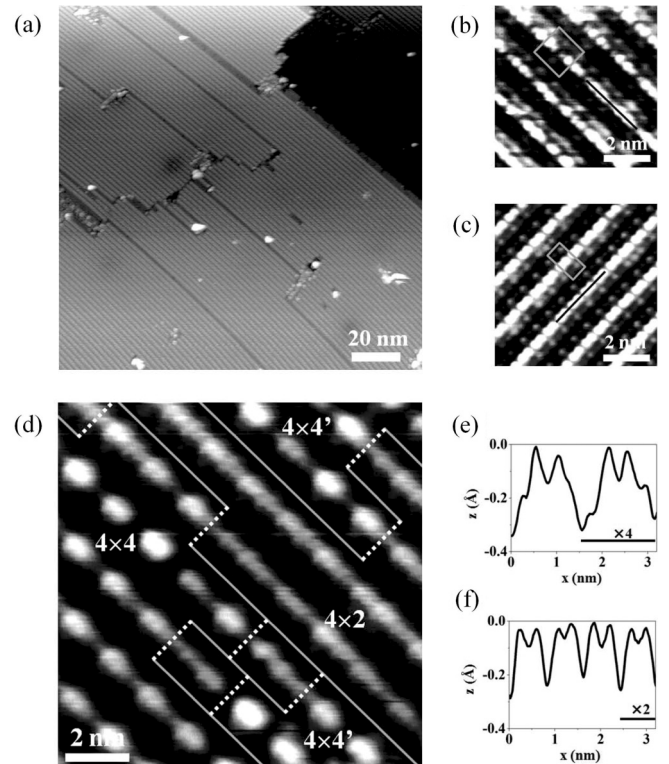


FIG. 2. (a) A large-scale STM image of Pt-induced nanowire arrays at room temperature ($I = 0.5$ nA, $V_S = -1.5$ V, 150×150 nm²). (b) and (c) Close-up STM images at 50 and 100 K, respectively ($I = 0.05$ nA, $V_S = -1.0$ V, 7×7 nm²). The gray boxes denote the unit cells. (d) A close-up STM image at 90 K ($I = 0.5$ nA, $V_S = -1.5$ V, 11×11 nm²). (e) and (f) Height profiles of the top dimers under the black solid lines in (b) and (c), respectively.

in the direction normal to the surface. The height difference is approximately 0.2 \AA . On the other hand, at 100 K, the height difference vanishes (i.e., each dimer is flat with respect to the horizontal axis). These two kinds of dimers are called “asymmetric” and “symmetric,” respectively, here. The above results agree with those reported by van Houselt *et al.*⁹

As shown in Fig. 2(d), at an intermediate temperature of 90 K, the $p(4 \times 2)$ and $p(4 \times 4)$ phases coexist in the same nanowires. In the $p(4 \times 4)$ phase, most of the neighboring dimers perpendicular to the nanowires are buckled in the same direction. Boundaries due to the antiphase patches are also seen (denoted as $4 \times 4'$). These boundaries often randomly move in the longitudinal direction of the nanowire during consecutive STM scans. The formation and motion of antiphase patches is less frequent at 50 K than those at 90 K. The formation of these antiphase patches seems to be the phase slipping assisted by a thermal lattice fluctuation effect. The features are very similar to those of quasi-1D metallic chains on In/Si(111) surfaces.^{25–27}

B. RHEPD rocking curves

Since the STM observations described above reveal that the low-temperature $p(4 \times 4)$ phase is responsible for the ground state of the Pt-induced nanowires on Ge(001) surface, we first determine its structure. Figure 3(a) shows the RHEPD rocking curve of the specular reflection spot at 35 K under the one-beam condition. Under this diffraction condition, the intensity of the diffraction spot depends mainly on interlayer distances and the atomic densities of the layers.²⁸

As described in the introduction, three structural models named PD, TDC, and NW are experimentally and theoretically proposed for the Pt-induced nanowires. The solid and broken lines plotted in Fig. 3(a) are the rocking curves calculated assuming the PD model, the TDC model, and the two NW models, while optimizing the atomic positions so as to minimize the reliability factor (R).²⁰ Under the assumptions of the PD model and the TDC model, the calculated curves exhibit dips at $\theta = 1.7^\circ$ and 1.4° , respectively, in the total reflection region, because of the interference effects of the positron waves reflected by the first and second surface layers.³⁰ This feature does not appear in the experimental curve. The overall shape of the calculated curves for both models is also not similar to the experimental data ($R = 4.6\%$ and 4.9%). Contrarily, the calculated curves for the NW models with a Pt coverage of 0.75 and 0.8125 ML are in good agreement with the experimental curve. Their reliability factors are 1.2%. We also examined other proposed structural models composed of the topmost Ge and/or Pt dimers with the Pt coverage ranging from $0.25 \sim 1 \text{ ML}$ in Refs. 10, 13, and 18. Among all the examined models, the two above-mentioned NW models with the topmost Ge dimers exhibit the lowest reliability factors.

Thus, the present results prefer the topmost Ge dimers rather than the Pt dimers. As for the CO adsorption,²⁹ a theoretical study suggests that Pt atoms in the second layer may act as adsorption sites.³¹ The local density of states near the Fermi level obtained through the STS measurements³² seem to agree with that theoretically predicted for the topmost Ge dimers.¹⁰

Figure 3(b) shows the rocking curve at 25 K in the many-beam condition. Solid and broken lines are the calculated curves for the NW models with a Pt coverage of 0.75 and

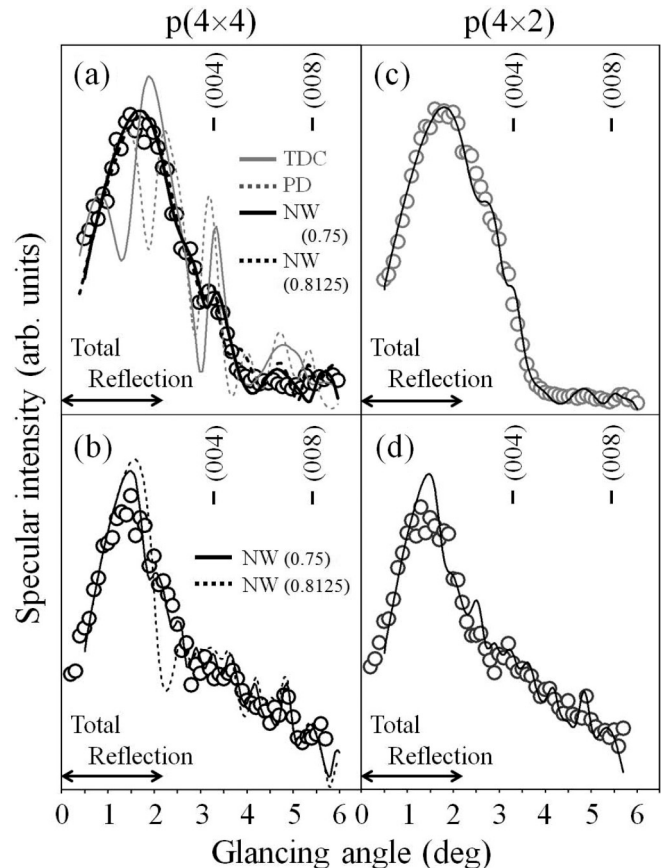


FIG. 3. (a) RHEPD rocking curves measured from Pt-induced nanowires on the Ge(001) surface under the (a) one-beam condition at 35 K, (b) many-beam condition at 25 K, (c) one-beam condition at room temperature, and (d) many-beam condition at room temperature. The open circles denote experimental data. The solid gray, broken gray, solid black, and broken black lines are the calculated curves for the TDC, PD, and (two) NW models with a Pt coverage of 0.75 and 0.8125 ML, respectively.

0.8125 ML, respectively. The NW model with a Pt coverage of 0.75 ML is in better agreement with the experimental data ($R = 1.8\%$) than is the NW model with a Pt coverage of 0.8125 ML ($R = 2.8\%$). In the latter model, additional Pt atoms occupying sites A shown in Fig. 1(b) result in the dip at $\theta = 2.3^\circ$. Thus, the fundamental structure of the Pt-induced nanowires may be explained by the NW model with a Pt coverage of 0.75 ML. The amount of evaporated Pt ($\sim 1.2 \text{ ML}$) is greater than 0.75 ML. The excess Pt atoms probably re-evaporate and/or diffuse into the bulk during the deposition.^{15,33,34}

Table I lists the optimized interlayer and interatomic distances [see Fig. 1(b)] obtained from the RHEPD experiments and the theoretical calculation.¹⁰ The experimental values nearly match those predicted theoretically. The RHEPD result suggests the presence of asymmetric Ge dimers ($a = 0.22 \pm 0.10 \text{ \AA}$), that is, adjacent Ge dimers are alternately buckled in the direction normal to the surface. The appearance of the $p(4 \times 4)$ periodicity is indeed explained by the asymmetric Ge dimers. This is consistent with the previously mentioned STM observations.

Figures 3(c) and 3(d) show the RHEPD rocking curves obtained at room temperature under the one-beam and

TABLE I. Interlayer and interatomic distances in the Pt-induced nanowire, as determined from the RHEPD rocking curve analysis. The labels a , b , c ($=\sqrt{c_{\parallel}^2 + c_{\perp}^2}$), and d are denoted in Fig. 1(b). Experimental errors are written in parentheses. For comparison, the theoretical values¹⁰ are also listed.

	a (Å)	b (Å)	c (Å)	d (Å)
Low temperature	0.22 (±0.10)	0.74 (±0.17)	3.4 (±0.2)	2.9 (±0.2)
High temperature	0.04 (±0.09)	0.64 (±0.15)	3.3 (±0.2)	2.9 (±0.2)
Theory	< 0.03	0.52	3.13	2.72

many-beam conditions. Figure 4(a) shows the comparison of the rocking curves under the one-beam condition at 35 K and room temperature for $\theta = 1^\circ$ – 4° . It can be seen from the figure that the intensity for the curve obtained at room temperature is higher than that for the curve obtained at 35 K as θ varies

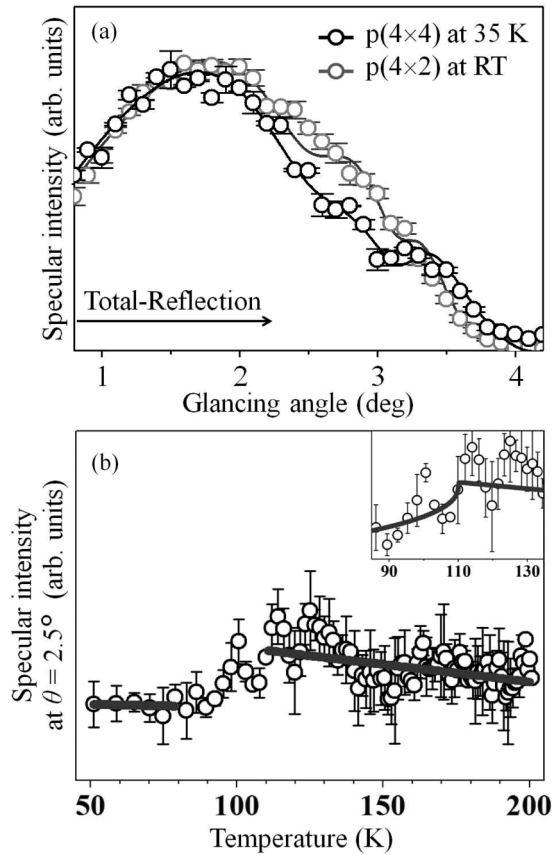


FIG. 4. (a) Comparison of the one-beam RHEPD rocking curves from Figs. 3(a) and 3(c). The black and gray open circles show the experimental data at 35 K and room temperature, respectively. The solid lines are the calculated curves for the NW model with a Pt coverage of 0.75 ML. (b) The temperature-dependent one-beam specular spot intensity curve at $\theta = 2.5^\circ$ for temperature range 50–200 K. The solid lines indicate the calculated temperature dependence assuming Debye temperatures of 210 and 130 K. The inset shows the closeup of the temperature dependence around T_c . The solid curve and solid line indicate the optimum temperature dependence below and above T_c , respectively.

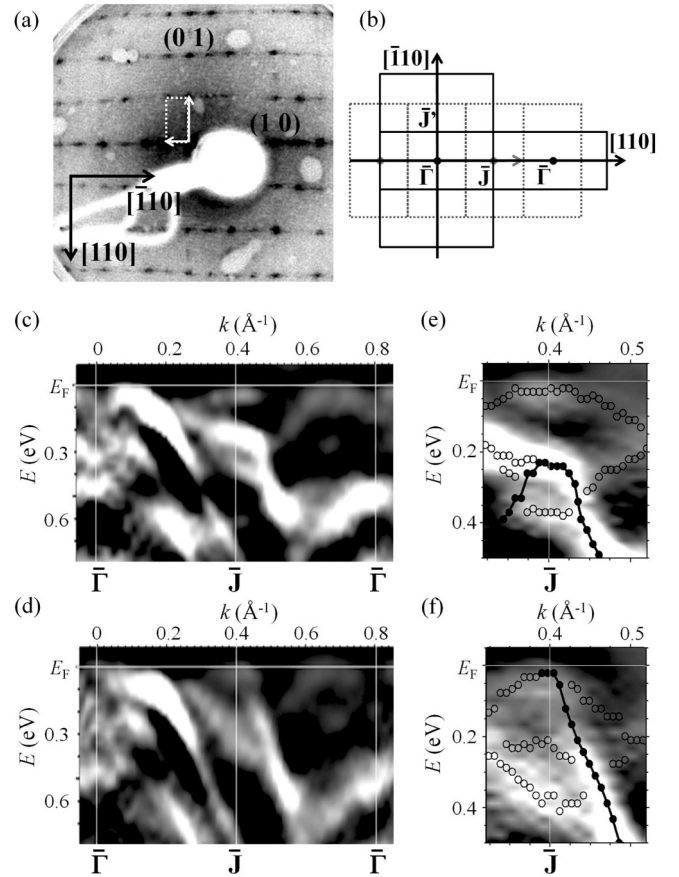


FIG. 5. (a) A LEED pattern from the Pt-induced nanowires on the vicinal Ge(001) substrate at room temperature. The energy of the incident beam is 80 eV. The dashed rectangle indicates the reciprocal unit cell. (b) The surface Brillouin zone of the $p(4 \times 2)$ unit cell. The solid and dashed lines represent the orthogonally rotated domains. (c) and (d) Second derivatives of ARPES spectra obtained at 65 K and room temperature, respectively. The photoemission intensity is greater in the brighter areas in gray scale. The white vertical lines denote the $\bar{\Gamma}$ and \bar{J} points. (e) and (f) Enlarged views of the areas around the \bar{J} point in (c) and (d), respectively. The solid and open circles represent the peak positions. E_F denotes the Fermi level.

from 2.3° to 3.2° . The solid lines in Figs. 3(c) and 4(a) are the calculated curves for the NW model with a Pt coverage of 0.75 ML after further optimization of the atomic positions. Consequently, as listed in Table I, at room temperature, the difference in height of the topmost Ge dimer atoms disappears ($a = 0.04 \pm 0.09$ Å). The rocking curve under the many-beam condition can also be explained by the symmetric Ge dimers.

Figure 4(b) shows the temperature dependence of the specular spot intensity for the one-beam condition at $\theta = 2.5^\circ$ in the temperature range 50–200 K. The intensity gradually increases from 80 to 110 K indicating the progress of the phase transition, and thereafter, a conventional Debye-Waller-like temperature dependence is observed within the experimental errors. From the slopes of the temperature-dependent specular intensity curve, the surface Debye temperatures are determined to be 210 ± 80 K for the low-temperature $p(4 \times 4)$ phase and 130 ± 40 K for the high-temperature $p(4 \times 2)$ phase. The amplitudes of the surface-normal vibrations²⁰ of the topmost Ge dimers are 0.06 Å at 50 K and 0.15 Å at 120 K.

Between 80 and 110 K, the above temperature dependence is somewhat continuous and would be reproduced by a power law, as shown by the inset in Fig. 4(b). The order parameter²¹ is proportional to $|1 - T/T_c|^\beta$ with $\beta = 0.36 \pm 0.15$ and $T_c = 111 \pm 10$ K. Although isolated nanowires⁹ existing at the domain boundaries alter the critical exponent, considering large enough domain areas of the present samples, such an effect is probably negligible. The value of the β (0.36) is smaller as compared to that anticipated for the mean-field approximation ($\beta = 0.5$). This is probably due to coexistences and fluctuations of the $p(4 \times 4)$, $p(4 \times 4')$, and $p(4 \times 2)$ phases as observed by STM in Fig. 2(d). In the present results with the STM observation in Fig. 2, the structural phase transition is very similar to a new type of phase transition,³⁵ that is, the precursory order-disorder behavior for the thermal fluctuating $p(4 \times 4)$ phase triggers the displacive transition from the $p(4 \times 4)$ phase to the $p(4 \times 2)$ phase.

C. Electronic band dispersions by ARPES

Figure 5(a) shows a typical low-energy electron diffraction (LEED) pattern from the Pt-induced vicinal substrate at room temperature. A double periodicity appears in the [110] direction with little sign of quadruple spots, whereas a quadruple periodicity prevails in the $[\bar{1}10]$ direction. These features suggest that most Pt-induced nanowires are aligned in the [110] direction. Thus, the Brillouin zones on the vicinal Pt/Ge(001) surface are single domains with a periodicity of $p(4 \times 2)$, as shown by solid rectangles in Fig. 5(b).

Figures 5(c) and 5(d) show the ARPES images taken along the [110] direction at 65 K and room temperature, respectively. In both images, the Ge bulk band appears at the center of the first surface Brillouin zone near the Fermi level, with parabolic dispersion toward the wave vector (k) $\sim 0.2 \text{ \AA}^{-1}$ and binding energy (E) of ~ 0.5 eV. Another bulk band dispersion³⁶ is seen from the $(k, E) \approx (0.1 \text{ \AA}^{-1}, 0.1 \text{ eV})$ to the $(k, E) \approx (0.4 \text{ \AA}^{-1}, 0.8 \text{ eV})$.

The dispersions around the \bar{J} point within the bulk band gap, as depicted in Figs. 5(e) and 5(f), are attributed to the surface state bands. There are the separable peaks denoted by open and solid circles by the peak-fitting procedure.³⁷ The dispersions denoted by open circles are nearly the same at 65 K and room temperature. Unfortunately, the origins of these bands are not known at present. One possible explanation might be the overlapping of the components of orthogonal minority domains.

The dispersions denoted by solid circles are probably related to the nanowires. The theoretical band dispersion for the NW model with a Pt coverage of 0.75 ML indeed explains the observed dispersion at room temperature. According to the theory behind that model,¹⁰ the band dispersion can be attributed to the bonding state between symmetric Ge dimers and the Pt atoms in the fourth layer as shown by the bottom Pt

atoms in Fig. 1(c). At 65 K, this dispersion shifts to a deeper region that is ~ 0.2 eV below the Fermi level. Similar behavior is also seen at the next \bar{J} point at $k = 1.2 \text{ \AA}^{-1}$, though it is not shown in the diagram. Considering the results of the STM and RHEPD experiments, the change in the band dispersion from 65 K to room temperature seems to be explained by the displacive transition from asymmetric to symmetric Ge dimers. The relatively high energetic gain of the asymmetric Ge dimer as compared to that of the theoretical value (~ 0.1 eV) on a Ge(001) surface³⁸ may indicate a contribution of the greater charge transfer from the lower atom to the higher atom of the asymmetric dimers.

The observed change of the STM image from $p(4 \times 2)$ to $p(4 \times 4)$ with fluctuating patches is consistent with the formation of charge density waves. The temperature dependence of the RHEPD intensity could also be interpreted as a Peierls transition associated with a thermal lattice fluctuation effect.³⁵ However, if a Peierls transition occurs, the width of a nesting vector at the Fermi level should appear to be $|k| = 0.4 \text{ \AA}^{-1}$ and not to be $|k| = 0.8 \text{ \AA}^{-1}$ as observed at the \bar{J} points. Therefore, we consider, the shift of the band dispersion at the \bar{J} points is probably due to the displacement of the topmost Ge dimers, but is not directly related to the Peierls transition. To discuss the possibility of the Peierls transition, more detailed ARPES experiments and theoretical calculations need to be performed.

IV. SUMMARY

We investigated the atomic configuration and electronic structure of the Pt-induced nanowires on a Ge(001) surface using STM, RHEPD, and ARPES. The structure of Pt-induced nanowires is very similar to that of a proposed theoretical NW model with a Pt coverage of 0.75 ML. However, the topmost Ge dimers are buckled to afford an asymmetric shape at low temperatures, and this explains the periodicity of the $p(4 \times 4)$ phase. At high temperatures, the asymmetric Ge dimers change to a symmetric flat structure. The above phase transition is explained as a displacive transition. We found that the shift of the band dispersion at the \bar{J} points is not directly related to a Peierls transition. To confirm the origin of the structural phase transition, more precise ARPES-based experiments are under progress.

ACKNOWLEDGMENTS

Some of the RHEPD experiments and all the ARPES experiments were carried out at the Slow Positron Facility, KEK Photon Factory, Japan (PF-PAC Grant No. 2010G652) and at BL-18A beamline, KEK Photon Factory, Japan (PF-PAC Grant No. 2010G649), respectively, under the approvals of the PF Program Advisory Committee. A part of this research was conducted under the auspices of Joint Development Research at High Energy Accelerator Research Organization (KEK).

*mochizuki.izumi@jaea.go.jp

¹P. C. Snijders and H. H. Weitering, *Rev. Mod. Phys.* **82**, 307 (2010).

²J. R. Ahn, J. H. Byun, J. K. Kim, and H. W. Yeom, *Phys. Rev. B* **75**, 033313 (2007).

³C. González, Jiandong Guo, J. Ortega, F. Flores, and H. H. Weitering, *Phys. Rev. Lett.* **102**, 115501 (2009).

⁴S. Hatta, Y. Ohtsubo, T. Aruga, S. Miyamoto, H. Okuyama, H. Tajiri, and O. Sakata, *Phys. Rev. B* **84**, 245321 (2011).

- ⁵J. N. Crain and F. J. Himpsel, *Appl. Phys. A* **82**, 431 (2006).
- ⁶C. Blumenstain, J. Schäfer, S. Mietke, S. Meyer, A. Dollinger, M. Lochner, X. Y. Cui, L. Patthey, R. Matzdorf, and R. Claessen, *Nature Phys.* **7**, 776 (2011).
- ⁷Changgan Zeng, P. R. C. Kent, Tae-Hwan. Kim, An-Ping Li, and Hanno H. Weitering, *Nature Mat.* **7**, 539 (2008).
- ⁸O. Gürlu, O. A. O. Adam, H. J. W. Zandvliet, and B. Poelsema, *Appl. Phys. Lett.* **83**, 4610 (2003).
- ⁹A. van Houselt, T. Gnielka, J. M. J. Aan de Brugh, N. Öncel, D. Kockmann, R. Heid, K. P. Bohnen, B. Poelsema, and H. J. W. Zandvliet, *Surf. Sci.* **602**, 1731 (2008).
- ¹⁰D. E. P. Vanpoucke and G. Brocks, *Phys. Rev. B* **81**, 085410 (2010).
- ¹¹D. E. P. Vanpoucke and G. Brocks, *Phys. Rev. B* **77**, 241308(R) (2008).
- ¹²A. A. Stekolnikov, F. Bechstedt, M. Wisniewski, J. Schäfer, and R. Claessen, *Phys. Rev. Lett.* **100**, 196101 (2008).
- ¹³A. A. Stekolnikov, J. Furthmüller, and F. Bechstedt, *Phys. Rev. B* **78**, 155434 (2008).
- ¹⁴J. Schäfer, D. Schrupp, M. Preisinger, and R. Claessen, *Phys. Rev. B* **74**, 041404(R) (2006).
- ¹⁵J. Schäfer, S. Meyer, C. Blumenstein, K. Roensch, R. Claessen, S. Mietke, M. Klinke, T. Podlich, R. Matzdorf, A. A. Stekolnikov, S. Sauer, and F. Bechstedt, *New J. Phys.* **11**, 125011 (2009).
- ¹⁶M. Fischer, A. van Houselt, D. Kockmann, B. Poelsema, and H. J. W. Zandvliet, *Phys. Rev. B* **76**, 245429 (2007).
- ¹⁷U. Schwingenschlögla and C. Schuster, *Eur. Phys. J. B* **60**, 409 (2007).
- ¹⁸U. Schwingenschlögla and C. Schuster, *EPL* **81**, 26001 (2008).
- ¹⁹A. Kawasuso, T. Ishimoto, M. Maekawa, Y. Fukaya, K. Hayashi, and A. Ichimiya, *Rev. Sci. Instr.* **75**, 4585 (2004).
- ²⁰Y. Fukaya, A. Kawasuso, K. Hayashi, and A. Ichimiya, *Phys. Rev. B* **70**, 245422 (2004).
- ²¹Y. Fukaya, A. Kawasuso, and A. Ichimiya, *Phys. Rev. B* **75**, 115424 (2007).
- ²²H. W. Yeom, Y. K. Kim, E. Y. Lee, K.-D. Ryang, and P. G. Kang, *Phys. Rev. Lett.* **95**, 205504 (2005).
- ²³P. Morgen, M. Szymonski, J. Onsgaard, B. Jørgensen, and G. Rossi, *Surf. Sci.* **197**, 347 (1988).
- ²⁴G. Radi, *Acta Crystallogr., sect. A: Cryst. Phys., Diffr., Theor. Gen. Crystallogr.* **26**, 41 (1970).
- ²⁵S. J. Park, H. W. Yeom, J. R. Ahn, and I.-W. Lyo, *Phys. Rev. Lett.* **95**, 126102 (2005).
- ²⁶J. Guo, G. Lee, and E. W. Plummer, *Phys. Rev. Lett.* **95**, 046102 (2005).
- ²⁷H. Morikawa, I. Matsuda, and S. Hasegawa, *Phys. Rev. B* **70**, 085412 (2004).
- ²⁸A. Ichimiya, *Solid State Phenom.* **28–29**, 143 (1992).
- ²⁹N. Oncel, W. J. van Beek, J. Huijben, B. Poelsema, and H. J. W. Zandvliet, *Surf. Sci.* **600**, 4690 (2006).
- ³⁰A. Kawasuso and S. Okada, *Phys. Rev. Lett.* **81**, 2695 (1998).
- ³¹D. E. P. Vanpoucke and G. Brocks, *Phys. Rev. B* **81**, 235434 (2010).
- ³²H. J. W. Zandvliet, A. van Houselt, and B. Poelsema, *J. Phys.: Condens. Matter* **21**, 474207 (2009).
- ³³O. Gürlu, H. J. W. Zandvliet, B. Poelsema, S. Dag, and S. Ciraci, *Phys. Rev. B* **70**, 085312 (2004).
- ³⁴H. J. W. Zandvliet, H. K. Louwsma, P. E. Hegeman, and B. Poelsema, *Phys. Rev. Lett.* **75**, 3890 (1995).
- ³⁵T. Aruga, *Surf. Sci. Rep.* **61**, 283 (2006).
- ³⁶K. Nakatsuji, Y. Takagi, F. Komori, H. Kusunohara, and A. Ishii, *Phys. Rev. B* **72**, 241308(R) (2005).
- ³⁷I. Mochizuki, R. Negishi, and Y. Shigeta, *J. Appl. Phys.* **106**, 013709 (2009).
- ³⁸H. J. W. Zandvliet, D. Terpstra, and A. van Silfhout, *J. Phys.: Condens. Matter* **3**, 409 (1991).